Chinese Journal of
POLYMER SCIENCE

RESEARCH ARTICLE

https://doi.org/10.1007/s10118-023-3046-8
Chinese J. Polym. Sci. **2024**, *42*, 239–246

Investigating the Absorption and Desorption Behavior of Methylene Chloride in the Poly(aryl ether ketone) Film with Different Crystallinities

Hong-Ru Yang, Jin-Dong Zhang, Dong-Ting Gao, Gang Liu, Chun-Hai Chen, and Jia-Nan Yao*

Center for Advanced Low-Dimension Materials, State Key Laboratory for Modification of Chemical Fibers and Polymer Materials, College of Materials Science and Engineering, Donghua University, Shanghai 201620, China

Electronic Supplementary Information

Abstract Poly(aryl ether ketone) (PAEK) films with different crystallinities were obtained by controlling the cooling rate, which were subjected to the absorption and desorption of methylene chloride (CH_2Cl_2). We employed attenuated total reflection Fourier transform infrared (ATR-FTIR) spectroscopy analyses to investigate the diffusion behavior of CH_2Cl_2 in PAEK films with different crystallinities. According to the Fickian diffusion model, the calculated diffusion coefficients of CH_2Cl_2 in PAEK films were observed to decrease with increasing crystallinity. The effect of CH_2Cl_2 absorption and desorption on the mechanical properties of PAEK films with different crystallinity was further analyzed using tensile tests. The tensile tests exhibited that CH_2Cl_2 has two concurrent effects: plasticization and solvent-induced crystallization. Differential scanning calorimetry (DSC) and wide-angle X-ray diffraction (WXRD) techniques further confirmed solvent-induced crystallization behavior. The results would be beneficial to understand the solvent resistance of PAEK materials and consequently provide the practical application conditions of PAEK with a theoretical basis.

Keywords Poly(aryl ether ketone); Diffusion behavior; Infrared spectra; Solvent-induced crystallization; Mechanical properties

Citation: Yang, H. R.; Zhang, J. D.; Gao, D. T.; Liu, G.; Chen, C. H.; Yao, J. N. Investigating the absorption and desorption behavior of methylene chloride in the poly(aryl ether ketone) film with different crystallinities. *Chinese J. Polym. Sci.* **2024**, *42*, 239–246.

INTRODUCTION

With the performance of thermoplastic matrix materials gradually improved, thermoplastic composites have attracted greater interest from the industry.[1,2] As a member of the thermoplastic family, poly(aryl ether ketone)s (PAEKs) have good impact resistance, high-temperature properties, and excellent mechanical properties, which show good applicability in the matrix material of aerospace structural composites.[3–5] As structural material in aeronautics, it is widely used as a matrix in carbon fiber reinforced composites in parts like wing flaps, access panels and floor panels, amongst others.[6–8] In high-performance applications, materials must be able to withstand a variety of aggressive environments.[9,10] One of them is exposure to various chemical solvents in the environment. Therefore, it is essential to understand the effects of solvent exposure on the morphology and properties of high-performance thermoplastic composites.

As a member of the PAEKs family, poly(ether ether ketone) (PEEK) is one of the most widely studied, and its solvent resistance has been extensively explored. The majority of these studies have focused on the absorption of highly interactive liquids and vapors into both amorphous and semi-crystalline PEEK samples. Penetrants of interest have included carbon disulfide, toluene, benzene, chloroform, and methylene chloride (CH_2Cl_2).[9–16] Among the various solvents studied, CH_2Cl_2 is of interest since CH_2Cl_2 is an active ingredient used in paint strippers and widely used in many applications, so it is essential to determine the effect of CH_2Cl_2 on the performance of PEEK. The equilibrium concentration of CH_2Cl_2 in PEEK is relatively high, with reported values varying from 15 wt% to 27 wt%. Arzak *et al*.[16] studied the sorption of CH_2Cl_2 by PEEK for both amorphous and highly crystalline polymers. They found that PEEK absorbed considerable amounts of CH_2Cl_2. The solvent sorption is faster for quenched film samples than for slowly cooled film samples. The equilibrium weight gain is also higher in quenched film samples. Stober *et al*.[17] reported that CH_2Cl_2 can be highly absorbed in the PEEK films, leading to two significant effects: plasticization and additional crystallization of incompletely crystallized films. Seferis *et al*.[18] reported that the initial crystallinity shows a pronounced effect on the kinetic and equilibrium absorption of CH_2Cl_2 in PEEK films. Hay and Kemmish[19] studied the diffusion of several halogenated compounds. They concluded that

* Corresponding author, E-mail: yjn@dhu.edu.cn

Received June 19, 2023; Accepted August 21, 2023; Published online September 19, 2023

those containing an activated hydrogen atom and an electronegative atom attached to the same carbon atom diffused most readily into PEEK and induced crystallization to a limited extent at room temperature. They also observed that partially crystallized PEEK was more resistant to solvent-induced crystallization (SIC) and penetrant diffusion into the polymer is slower.

However, PEEK has the highest ether/ketone ratio in the PAEKs family, which requires higher processing temperatures as a consequence of the material's melting temperature and viscosity, making its application somewhat limited.[20] Therefore, excellent mechanical properties and lower processing temperature than PEEK make PAEK an interesting candidate for high-performance applications as well.[21,22] Compared to PEEK, very limited work is reported on the solvent resistance of PAEK and the above studies on the diffusion behavior of CH_2Cl_2 in PEEK generally used the static gravimetric method. This technique is labor intensive since the samples must be taken out of the testing environment at various time and over a long period for external weighing. Moreover, the handling time outside the test environment can be a significant source of error.[23] To overcome these limitations, another technique used in the study is the attenuated total reflection-Fourier transform infrared (ATR-FTIR), which has been proven to be an effective means of tracking the diffusion behavior of small molecules in the polymer matrix.[24]

Through ATR-FTIR spectroscopy, plentiful information about the diffusion coefficient and the interactions between small molecules and the polymer matrix can be obtained.[25,26] Moreover, it does not need special processing steps or do any damage to samples during testing.[27,28] Hou *et al.*[29] monitored the water diffusion processes in the EC-based films containing different amount of TEC using time-resolved ATR-FTIR spectra. On the basis of Fickian diffusion model, the water diffusion coefficients in different films be evaluated from the resulting diffusion spectra. It is demonstrated that the diffusion coefficient increases with increasing TEC content, which parallels with the fact that higher TEC content could create more free volume in the EC matrix and thus make it easier for water to diffuse. Sammon *et al.*[30] used the ATR-FTIR technique to explore the diffusion of methanol in PET with varying degrees of crystallinity, finding that the diffusion coefficient decreased with increasing the degree of crystallinity. Yang *et al.*[31] studied the diffusion behavior of urea aqueous solution with different concentrations (0 wt% (water), 20 wt%, 40 wt%, 50 wt%) in viscose fiber membrane by using ATR-FTIR spectroscopy. According to the Fick diffusion model, the diffusion coefficient of urea molecules in viscose fiber membrane decreases with the increase of urea concentration.

Up to now, to the best of our knowledge, research by FTIR spectroscopy aiming at studying the diffusion behavior of CH_2Cl_2 in PAEK films of different crystallinity has been scarcely reported. Therefore, in this work, the diffusion behavior of CH_2Cl_2 in different crystalline PAEK films was investigated by ATR-FTIR spectroscopy. Moreover, the mechanical properties of PAEK films with different crystallinity after CH_2Cl_2 absorption and desorption were tested, which can be used to measure the solvent resistance of PAEK. Furthermore, this work compared the solvent resistance properties of PAEK with traditional commercial PEEK. The results would be beneficial to understand the solvent resistance of PAEK materials and consequently provide the practical application conditions of PAEK with a theoretical basis.

EXPERIMENTAL

Raw Materials

PAEK and PEEK were provided by Hairuite Engineering Plastics Co., Ltd. in the form of grain. The resin used in this work is a new type of PAEK independently developed and the mechanical properties of PAEK are similar to those of conventional commercial PEEK. Table S1 and Fig. S1 (in the electronic supplementary information, ESI) show the details of the PAEK. However, it has a higher glass transition temperature (T_g) and lower melting temperature, which facilitates the molding and processing of thermoplastic composites. CH_2Cl_2 was purchased from Adamas-Reagent without further purifications.

Preparation of Films with Different Crystallinities

The films with different crystallinities were prepared as shown in Fig. 1. In the lower cavity of the mold, 3 g of PAEK powder was weighed and spread evenly, and the effective inner size of the cavity was 100 mm × 100 mm. After the mold was closed, it was placed in a hot press heated to 360 °C and subjected to a pressure of 2 MPa. The temperature was held for 10 min and then cooled to room temperature in different ways. Amorphous (AM) PAEK films were obtained by quenching in liquid nitrogen, low crystallinity (LC) PAEK films were obtained by quenching in normal water, and high crystallinity (HC) PAEK films were obtained by cooling slowly in a hot press. The crystallinity of the AM-PAEK, LC-PAEK and HC-PAEK films was measured by DSC and was 0%, 8% and 33%, respectively.

Absorption and Desorption

Absorption was performed by immersing PAEK films in a closed container containing CH_2Cl_2 at room temperature until

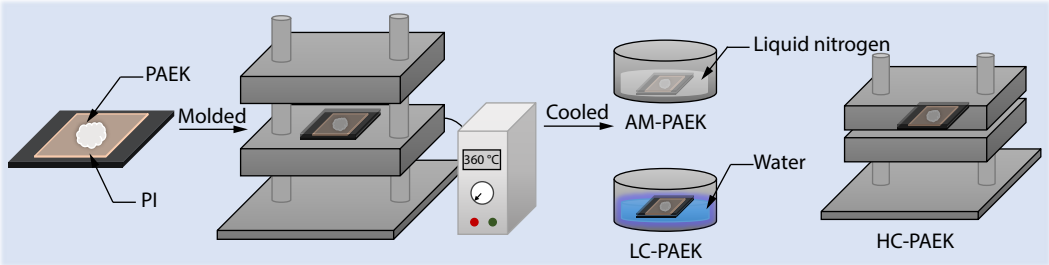

Fig. 1 Schematic illustration of the preparation of films with different crystallinities.

https://doi.org/10.1007/s10118-023-3046-8

absorption equilibrium. Desorption was performed by putting the PAEK films in a vacuum at 140 °C, above the boiling point of CH_2Cl_2 (39.8 °C) but well below the T_g of PAEK (152 °C). This desorption method allows the drying of the sample without inducing further crystallization or other structural changes. The percentage of solvent in the samples was calculated from Eq. (1):

$$\text{Solvent} = \frac{W_a - W_i}{W_i} \times 100\% \quad (1)$$

where W_a is the weight after absorption or desorption, W_i is the initial weight.

Characterization

ATR-FTIR diffusion

All the time-resolved ATR-FTIR spectra were collected on a Nicolet iS50 FTIR spectrometer equipped with a DTGS detector. To collect the ATR-FTIR spectra at the initial stage of the diffusion process, 8 scans at a resolution of 4 cm^{-1} were accumulated. The spectral data were collected with an interval time of 6 s. The schematic illustration of the diffusion experiment by ATR-FTIR spectroscopy is shown in Fig. 2. The polymer matrix is located between the ATR crystal and the diffusion substance. The diffusion substance is detected when it diffuses from the upper surface of the polymer matrix to the lower surface. As time increases, the intensity of the characteristic absorption band associated with the diffusing substance gradually increases until diffusion reaches equilibrium. The diffusion curve can be obtained by taking the diffusion time as the abscissa and the characteristic absorption peak intensity/area of the diffusion substance as the ordinate.

The Fickian diffusion equation by Fieldson and Barbari[24] is handy for estimating the diffusion coefficient of small molecules in polymer films from ATR-FTIR data.

$$\frac{A_t}{A_\infty} = 1 - \frac{8\gamma}{\pi[1-\exp(-2L\gamma)]} \cdot \sum_{n=0}^{\infty}\left[\frac{\exp(g)\left[\exp(-2L\gamma)+(-1)^n(2\gamma)\right]}{(2n+1)\left(4\gamma^2+f^2\right)}\right] \quad (2)$$

$$g = \frac{-D(2n+1)^2\pi^2 t}{4\gamma L^2} \quad (3)$$

$$f = \frac{(2n+1)\pi}{2L} \quad (4)$$

$$\gamma = \frac{2n_2\pi\sqrt{\sin^2\theta - \left(\frac{n_1}{n_2}\right)^2}}{\lambda} \quad (5)$$

where γ is the penetration depth of the evanescent wave; θ (θ=45°) is the angle of the incidence of infrared (IR) radiation; n_1 and n_2 are the refractive indexes of the polymer film and the ATR crystal, respectively.

Eq. (2) can be simplified by eliminating all terms in the series after the first:[29]

$$\frac{A_t}{A_\infty} = 1 - \frac{8\gamma}{\pi[1-\exp(-2L\gamma)]} \cdot \frac{[f\cdot\exp(-2L\gamma)+(2\gamma)]}{\left(4\gamma^2+f^2\right)} \cdot \exp(g) \quad (6)$$

γ is assumed to be a constant, and L is 60 μm; therefore, Eq. (7) can be reduced to the expression:

$$A_t = A_\infty - A' \cdot \exp(g) \quad (7)$$

where $A' = A_\infty \cdot \frac{8\gamma}{\pi[1-\exp(-2L\gamma)]} \cdot \frac{[f\cdot\exp(-2L\gamma)+(2\gamma)]}{\left(4\gamma^2+f^2\right)}$.

Thus, by a nonlinear curve fitting to Eq. (7) from the ν_{C-Cl} band intensities of CH_2Cl_2 in the difference spectra versus time, the diffusion coefficient can be obtained in which $D = \frac{-4L^2(g/t)}{\pi^2}$.

Mechanical properties

With ASTM D882 as a reference,[32] the tensile properties of the PAEK films were tested using an Instron 5966 1-kN Universal Testing Machine (Instron, USA). The nominal size of the specimen is 50 mm × 5 mm × (0.05±0.005) mm. The average values of five parallel samples' tensile strength (σ) and Young's modulus (E) are taken, respectively.

Differential scanning calorimetry (DSC)

The crystallization behavior of the samples was characterized using a differential scanning calorimeter (DSC, Q250, TA Instruments). The samples (5–10 mg) were heated from 50 °C to 400 °C at 10 °C/min in a nitrogen atmosphere. The absolute crystallinity (X_c) of the thermoplastic can be calculated by Eq. (8):[33]

$$X_c = \frac{\Delta H_c}{\Delta H_f^0} \times 100\% \quad (8)$$

where ΔH_c is estimated by integrating the area under the melting peak. The theoretical melting enthalpy (ΔH_f^0) of completely crystallized PAEK and PEEK is taken as 130 J/g.[34]

Wide-angle X-ray diffraction (WXRD)

WXRD was collected by the Denki D/MAX-2500 rotary target X-ray diffractometer of Rigaku Company at room temperature.

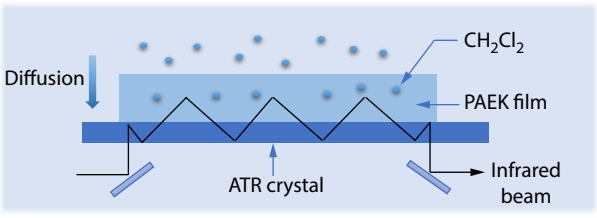

Fig. 2 Schematic illustration of the diffusion experiments by ATR-FTIR spectroscopy.

RESULTS AND DISCUSSION

Absorption and Desorption

The absorption and desorption data are summarized in Fig. 3. It can be found that CH_2Cl_2 is readily absorbed by PAEK films, especially in AM-PAEK and LC-PAEK films, where the weight after absorption equilibrium reaches 26.9±1.2 wt% and 23.5±2.3 wt%, respectively. HC-PAEK film still has 10.9±0.8 wt% absorption. A large amount of absorption gave rise to the study of the diffusion process of CH_2Cl_2 in PAEK films, which was investigated in this work using an infrared method. Meanwhile, it is interesting to note that AM-PAEK and LC-PAEK films were found to become immediately opaque during the absorption process, revealing the SIC phenomenon, which has also been observed in previous studies.[19] To further discern the effects of SIC and plasticization resulting from CH_2Cl_2 absorption, desorption experiments were performed to remove as much

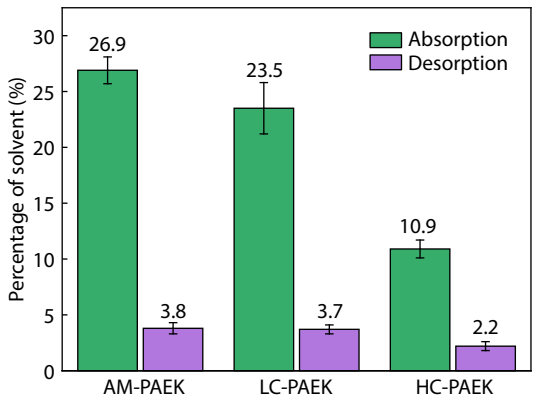

Fig. 3 The sorption and desorption data for CH_2Cl_2 from PAEK.

CH_2Cl_2 as possible to exclude the effects of plasticization. After desorption, the CH_2Cl_2 content in PAEK films was reduced by 23.1±1.7 wt%, 19.8±2.7 wt% and 8.7±1.2 wt%, respectively. However, some residual CH_2Cl_2 solvent remained in the PAEK film even after the equilibrium of weight loss was recorded at 150 °C, indicating the absorption process's lack of complete reversibility.

Evaluation of CH_2Cl_2 Diffusion Coefficients in PAEK

Infrared spectroscopy was used to study the diffusion process of CH_2Cl_2 in PAEK films with different crystallinities. The ATR-FTIR spectra of the PAEK film and CH_2Cl_2 collected are shown in Fig. 4. As observed, the characteristic bands of CH_2Cl_2, such as ν_{C-Cl}, are located in the region of 800–650 cm^{-1}, which is less overlapped with bands of the PAEK film. Under such a circumstance, this region will be mainly focused on investigating the diffusion process of CH_2Cl_2 in the PAEK film.

The diffusion behavior of CH_2Cl_2 in different crystallinity PAEK films was monitored by ATR-FTIR spectroscopy. The obtained diffusion spectra in the region of 800–650 cm^{-1} are shown in Fig. 5. It is noted that almost all the bands are closely related to solution diffusion and regularly change in intensity. Herein, the broad band in the region of 780–750 cm^{-1} is constituted of C—H out-of-plane bending vibration of PAEK molecules and ν_{C-Cl} stretching vibration of CH_2Cl_2 molecules. The ν_{C-Cl} stretching vibration is affected by PAEK molecules. To some extent, it is relatively difficult to study the diffusion process of CH_2Cl_2 in the PAEK film by analyzing this

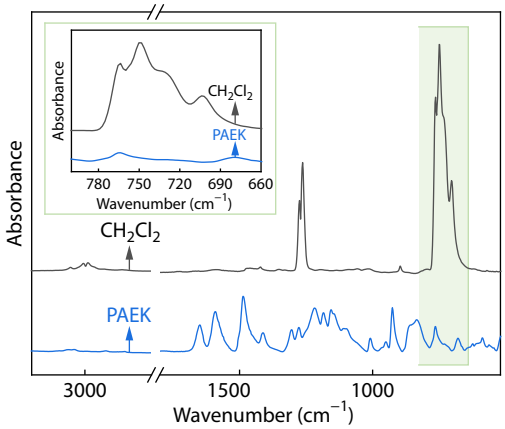

Fig. 4 ATR-FTIR spectra of PAEK film and CH_2Cl_2.

region. Furthermore, the intensities of bands at 732 cm^{-1} can reflect the diffusion process of CH_2Cl_2 molecules much more clearly. As observed, the intensities of bands at 732 cm^{-1}, which are related to ν_{C-Cl} stretching vibration, increase remarkably during the diffusion process, indicating the diffusion of CH_2Cl_2 through the PAEK films. Moreover, considering the effect of crystallinity on the diffusion process, it can be noticed that higher crystallinity leads to slower diffusion.

For a better understanding of the diffusion behavior, diffusion curves of CH_2Cl_2 in the PAEK film are illustrated in Fig. 6.

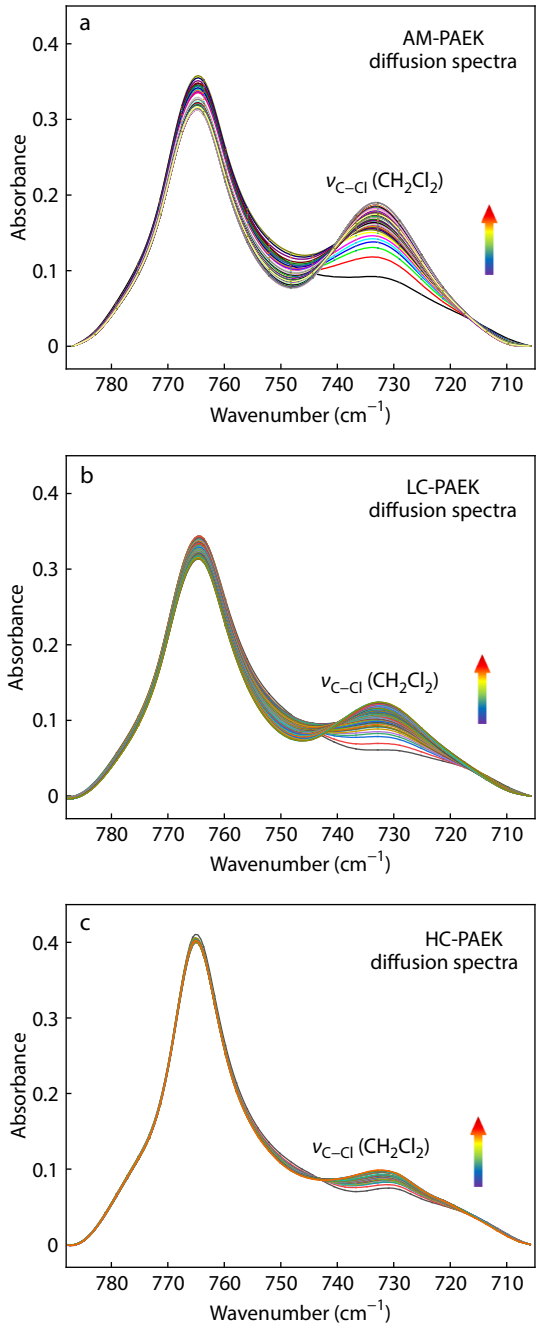

Fig. 5 Time-resolved ATR-FTIR spectra collected during CH_2Cl_2 diffusion in different crystallinities: (a) AM-PAEK, (b) LC-PAEK, and (c) HC-PAEK.

https://doi.org/10.1007/s10118-023-3046-8

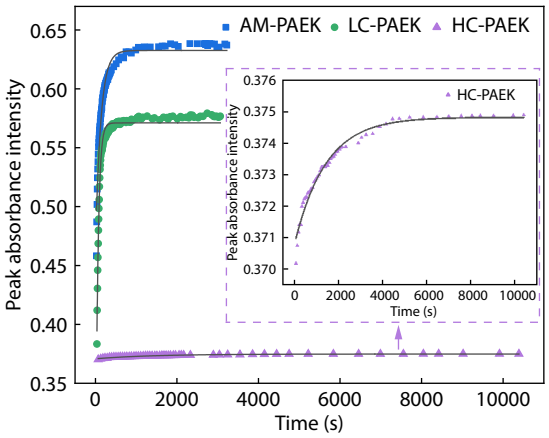

Fig. 6 The peak absorbance intensity of the ν_{C-Cl} region during CH_2Cl_2 diffusing in the different crystallinity PAEK film. Experimentally collected data and mathematically simulated curve (black line).

Herein, the peak absorbance intensity of ν_{C-Cl} is plotted as a function of diffusion time. In Fig. 6, the points represent the experimental data and the solid lines are simulated by nonlinear curve fitting based on Eq. (3). It is demonstrated that the above diffusion curves accord well with the Fickian diffusion model.

The obtained diffusion coefficients are listed in Table 1. It can be found that the diffusion coefficient decreases with the crystallinity of the PAEK film increases. For AM-PAEK, the molecules are loosely packed, intermolecular interactions are weaker, and solvent molecules penetrate more easily into the interior of the polymer, so the diffusion coefficient is relatively high. Although LC-PAEK is partially crystallized compared with AM-PAEK, the molecular chains of the samples are still mainly irregularly ordered, and the intermolecular stacking is relatively loose, facilitating the diffusion of solvent and making it easy for solvent molecules to penetrate into the molecules. The crystallinity of HC-PAEK is further improved compared with LC-PAEK, and the molecular chains are regularly and tightly arranged, while intermolecular interactions exist, making it relatively difficult for solvent molecules to penetrate it, and its diffusion coefficient is relatively minimal.

Table 1 Diffusion coefficients of CH_2Cl_2 in the different crystallinity PAEK film.

Sample	D ($cm^2 \cdot s^{-1}$)
AM-PAEK	7.1×10^{-12}
LC-PAEK	3.2×10^{-12}
HC-PAEK	6.6×10^{-13}

Mechanical Properties

Table 2 presents a summary of the tensile properties for all specimens under dry, absorption and desorption conditions. As would be expected from the DSC results, the high crystallinity with ordered crystallites obtained at a low cooling rate gave rise to a high tensile strength and Young's modulus of PAEK films. The effect of the absorption of CH_2Cl_2 on the performance of AM-PAEK, LC-PAEK and HC-PAEK was evident, with all samples showing a decrease in stress-related performance compared to the initial values. The largest decrease was in the AM-PAEK sample, which showed a decrease in tensile strength of about 26% and a decrease in modulus of about 23%. For the LC-PAEK sample with 8% crystallinity, the tensile strength decreased by about 24% and the modulus decreased by about 18%, a reduced decrease relative to AM-PAEK, but still at a high level. The HC-PAEK sample with the highest crystallinity of 33% also showed a decrease in tensile strength of about 20% and a decrease in modulus of about 16%. The decrease in tensile strength and Young's modulus of PAEK films increased with the increase in absorption equilibrium. The marked decrease in these properties indicates a robust plasticizing effect of CH_2Cl_2 in PAEK.

It is also worth noting that the presence of CH_2Cl_2 may have two concurrent effects: the plasticization and the crystallization of PAEK due to the presence of small solvent molecules. It must be taken into account that the overall effect of these two effects on properties is opposite and while plasticization due to the presence of solvents in PAEK may be a rather reversible process, the induction of crystallization is not. Therefore, it is necessary to test the mechanical properties of PAEK films after desorption, which will provide helpful information on SIC.

Additional analysis reveals that the mechanical testing results of HC-PAEK films are more informative about the effects of SIC and plasticization since the SIC of HC-PAEK is almost negligible. Thus, the observed changes will be due only to the presence of CH_2Cl_2. From the mechanical properties of the HC-PAEK films, the CH_2Cl_2 solvent is a plasticizer because all the reported properties related to stress decrease as the solvent content increases. The effects of the decrease in solvent content after desorption on HC-PAEK agree with the above considerations because behavior opposite to that observed for absorption is now shown in all the properties. Thus, the mechanical properties of the HC-PAEK films before and after desorption indicate the lack of significant SIC in the initially highly crystalline PAEK. The presence of SIC in AM-PAEK and LC-PAEK films after desorption resulted in an increase in their tensile strength and Young's modulus. The above mechanical properties results agree with the results of DSC and

Table 2 Summary of tensile strength and Young's modulus of PAEK and PEEK samples obtained after absorption and desorption.

		PAEK			PEEK		
		AM-PAEK	LC-PAEK	HC-PAEK	AM-PEEK	LC-PEEK	HC-PEEK
Tensile strength (MPa)	Untread	57±2	59±3	79±9	54±5	58±4	83±4
	Equilibrium	42±3	45±4	63±6	40±3	48±2	62±7
	Desorption	71±3	75±2	84±2	69±4	76±2	78±9
Young's modulus (MPa)	Untread	2.2±0.1	2.2±0.2	3.0±0.1	2.3±0.1	2.3±0.1	3.2±0.1
	Equilibrium	1.7±0.1	1.8±0.2	2.5±0.2	1.8±0.1	1.8±0.2	2.6±0.2
	Desorption	2.3±0.2	2.3±0.1	3.0±0.1	2.4±0.1	2.5±0.1	3.2±0.1

https://doi.org/10.1007/s10118-023-3046-8

WXRD. The behavior of the mechanical properties after absorption and desorption of CH_2Cl_2 by AM-PAEK, LC-PAEK, and HC-PAEK allow us to discern the concomitant effects of SIC and plasticization on the mechanical properties of PAEK-containing sorbed CH_2Cl_2.

Moreover, Table 2 compares the solvent resistance properties of PAEK with traditional commercial PEEK. Again, the tensile strength and Young's modulus of PEEK films increased with crystallinity, and the mechanical properties of PEEK films were reduced by the absorption of CH_2Cl_2 and recovered or improved after desorption. On the basis of above data, it can be concluded that PAEK has a solvent resistance property similar to traditional commercial PEEK within the crystallinity studied herein. However, PAEK has a higher glass transition temperature and lower melting temperature than PEEK, resulting in a wider process window, which benefits the molding and processing of thermoplastic composites and thus is becoming more and more attractive.

Differential Scanning Calorimetry Analysis

DSC was used further to study the SIC behavior of CH_2Cl_2 in PAEK films. The DSC thermograms of PAEK films obtained by initially different cooling methods and after their absorption of CH_2Cl_2 are given in Fig. 7. For the convenience of discussion, the calculated crystallinity data are summarized in Table 3. It can be seen that heat flow curves under the liquid nitrogen (AM-PAEK) cooling and water (LC-PAEK) cooling strategies have obvious exothermic peaks in the range of 160–220 °C. For AM-PAK, the crystallinity formed by crystallization during the scan was about 19%, the crystallinity calculated from the melting endotherm was about 22%, and the 3% difference can be considered as the crystallinity present in the sample at room temperature. Similar to PEEK, within the margin of error for determining the enthalpy area, the PAEK melt-quenched sample is almost amorphous at room temperature and all crystallites are formed during the DSC scan.[35] The crystallinity of LC-PAEK calculated by calculating the difference between the crystallization enthalpy area and the melt inclusion area is about 8%. The HC-PAEK sample cooled in the furnace has no more cold crystallization peaks. In this case, the endotherms are very broad, with a distinct shoulder at about 297 °C and a sharp melting peak at 323 °C. The crystallinity of HC-PAEK calculated by the melt enthalpy area is about 33%. The crystallinity obtained from DSC is also in good conformity with the cooling rate.

The SIC produced by CH_2Cl_2 resulted in the disappearance of the exothermic crystallization peak for both AM-PAEK and LC-PAEK samples, while the melting peak was still present with an enthalpy of melting of about 40 J/g. The crystallinity of AM-PAEK and LC-PAEK samples was calculated to be about 31% based on the melting enthalpy, which increased by 31% and 26% after solvent adsorption, respectively. The crystallinity of HC-PAEK was essentially unchanged before and after adsorption and was about 33%. SIC was essentially absent in HC-PAEK, as the DSC curves were not significantly different in the initial HC-PAEK and CH_2Cl_2 exposed film samples, and the melting peaks and areas were essentially unchanged, which also corresponded to the mechanical results.

Wide-angle X-ray Diffraction Analysis

WXRD tests were conducted to gain deeper insights into the differences between the PAEK films obtained by SIC and thermal crystallization and the results are shown in Fig. 8. The initial AM-PAEK samples displayed a very broad amorphous hump. The relatively low crystallinity of the LC-PAEK samples

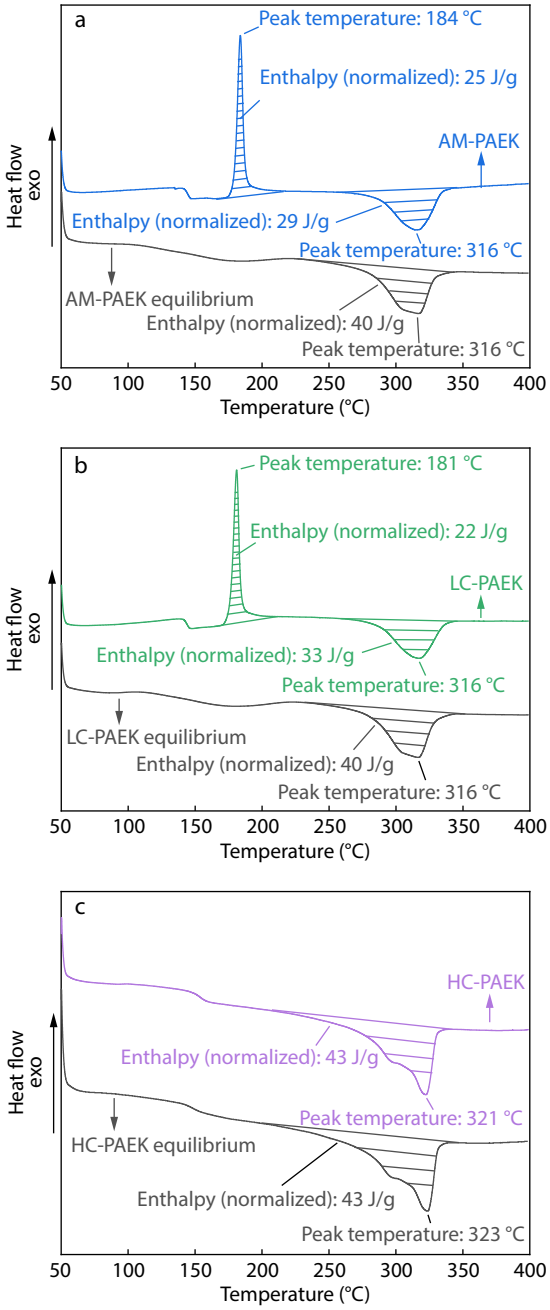

Fig. 7 DSC curves of the initial and CH_2Cl_2 exposed samples: (a) AM-PAEK, (b) LC-PAEK, and (c) HC-PAEK.

Table 3 Summary of the calculated crystallinity data for all samples.

Sample		X_c (%)
AM-PAEK	Untread	3
	Equilibrium	26
LC-PAEK	Untread	8
	Equilibrium	27
HC-PAEK	Untread	29
	Equilibrium	30

https://doi.org/10.1007/s10118-023-3046-8

with peak point 2θ=18.6° was challenging to detect by XRD and showed very broad amorphous humps. The initial HC-PAEK samples showed WXRD peaks at diffraction angles 2θ=19.1°, 21.1°, 23.4°, and 29.2°, associated with diffraction from the (110), (111), (200), and (211) crystallographic planes of form I, respectively. The (110) and (200) peaks are the strongest, indicating that crystallization occurs mainly along these two planes.[36,37] The AM-PAEK samples after absorption show several small peaks and shoulder peaks on the amorphous halo with angular positions roughly consistent with those found in the initially thermally crystalline HC-PAEK. The presence of crystalline peaks in the WXRD pattern also confirmed the existence of SIC by CH_2Cl_2 in the specimens. Similarly, the same phenomenon was observed in the LC-PAEK sample. Although the crystallinity of LC-PAEK samples improved compared to AM-PAEK but remained at a low level, CH_2Cl_2 produced induced crystallization in them, which was the same as the DSC results. And these crystalline peaks are less intense than those of thermally crystallized specimens, but the scattering angles at which they occur correspond to the scattering angles at which the crystalline peaks of thermally crystallized samples occur.

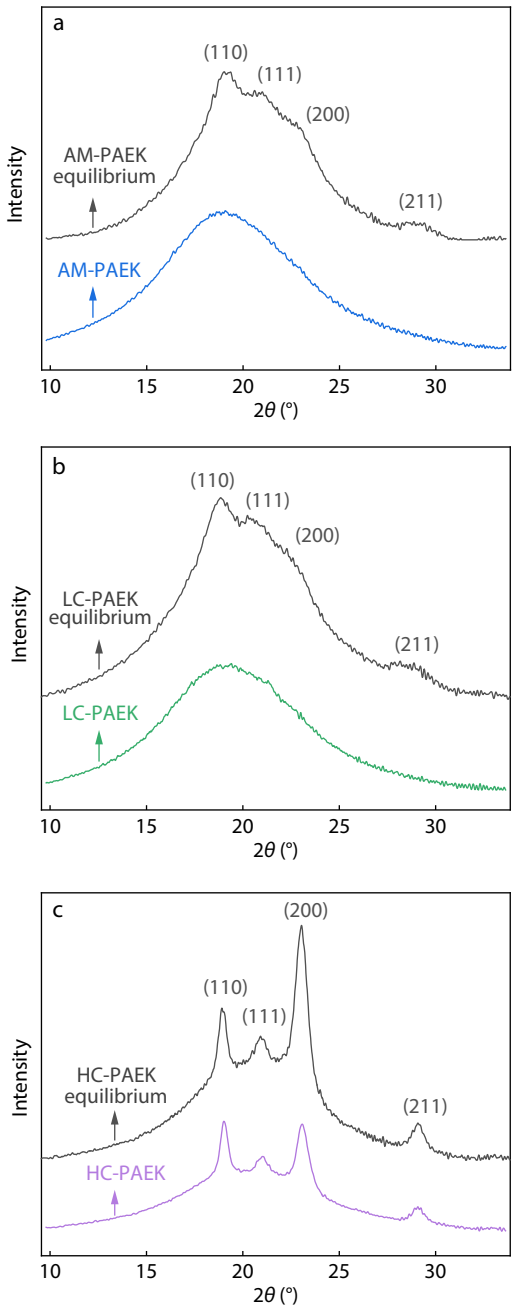

Fig. 8 WXRD patterns of PAEK after CH_2Cl_2 absorption and desorption: (a) AM-PAEK, (b) LC-PAEK, and (c) HC-PAEK.

CONCLUSIONS

In this study, the diffusion behavior of CH_2Cl_2 in the PAEK films with different crystallinities were studied by ATR-FTIR spectroscopy. The time-resolved ATR-FTIR spectra obtained during the diffusion process were used to create the diffusion profiles, which closely match the Fickian diffusion model. The diffusion coefficients of CH_2Cl_2 in PAEK films of different crystallinities can be evaluated. It is observed that the diffusion coefficient decreases with increasing crystallinity. The absorption of solvents has an important effect on the mechanical properties of the PAEK films. These effects result from the concomitant processes of plasticization by the solvents and SIC. The behavior of SIC was further confirmed using wide-angle X-ray diffraction and differential scanning calorimetry. Herein, the information obtained about the diffusion system might be helpful for us to understand better the effects of CH_2Cl_2 absorption on the properties of PAEK and further may be beneficial to analyze and understand PAEK matrix-dominated properties in the thermoplastic composite with reusability.

Conflict of Interests

The authors declare no interest conflict.

Electronic Supplementary Information

Electronic supplementary information (ESI) is available free of charge in the online version of this article at http://doi.org/10.1007/s10118-023-3046-8.

ACKNOWLEDGMENTS

We gratefully acknowledge Sheng-tong Sun and Lei Hou of Donghua University for their help in the infrared testing and analysis and article writing. This work was financially supported by the National Key R&D Program of China (No. 2022YFB3709402).

REFERENCES

1 Limaye, M.; Pradeep, S. A.; Kothari, A.; Savla, S.; Agha, A.; Pilla, S.; Li, G. Thermoforming process effects on structural performance of carbon fiber reinforced thermoplastic composite parts through a manufacturing to response pathway. *Compos. B Eng.* **2022,** *235*, 109728.
2 Veenstra, S. W. P.; Wijskamp, S.; Rosić, B.; Akkerman, R. Bending behaviour of thermoplastic composites in melt: a data-driven

approach. *Compos. Sci. Technol.* **2022,** *219*, 109220.
3 Hassan, E. A. M.; Ge, D. T.; Yang, L. L.; Zhou, J. F.; Liu, M. X.; Yu, M. H.; Zhu, S. Highly boosting the interlaminar shear strength of CF/PEEK composites *via* introduction of PEKK onto activated CF. *Compos. Part A Appl. Sci. Manuf.* **2018**, *112*, 155–160.
4 Cortes, L. Q.; Caussé, N.; Dantras, É.; Lonjon, A.; Lacabanne, C. Morphology and dynamical mechanical properties of poly ether ketone ketone (PEKK) with *meta* phenyl links. *J. Appl. Polym. Sci.* **2016**, *133*, 1–10.
5 Mazur, R. L.; Oliveira, P. C.; Rezende, M. C.; Botelho, E. C. Environmental effects on viscoelastic behavior of carbon fiber/PEKK thermoplastic composites. *J. Reinf. Plast. Compos.* **2014**, *33*, 749–757.
6 Gombos, Z. J.; McCutchion, P.; Savage, L. Thermo-mechanical behaviour of composite moulding compounds at elevated temperatures. *Compos. B Eng.* **2019,** *173*, 106921.
7 Karsli, N. G.; Demirkol, S.; Yilmaz, T. Thermal aging and reinforcement type effects on the tribological, thermal, thermomechanical, physical and morphological properties of poly(ether ether ketone) composites. *Compos. B Eng.* **2016**, *88*, 253–263.
8 Pérez-Martín, H.; Mackenzie, P.; Baidak, A.; Ó Brádaigh, C. M.; Ray, D. Crystallinity studies of PEKK and carbon fibre/PEKK composites: a review. *Compos. B Eng.* **2021**, *223*, 109127.
9 Arzak, A.; Eguiazabal, J. I.; Nazabal, J. The effects of solvent sorption on the properties of poly(ether ether ketone). *J. Mater. Sci.* **1993**, *28*, 3272–3276.
10 Wolf, C. J.; Bornmann, J. A.; Grayson, M. A.; Anderson, D. P. Solvent-induced crystallinity in poly(aryl-ether-ether-ketone) [PEEK]. *J. Polym. Sci., Part B: Polym. Phys.* **1992**, *30*, 251–257.
11 Grayson, M. A.; Wolf, C. J. The solubility and diffusion of water in poly(aryl-ether-ether-ketone) (PEEK). *J. Polym. Sci., Part B: Polym. Phys.* **1987**, *25*, 31–41.
12 Grayson, M. A.; Wolf, C. J. The effect of morphology on the transport of dichloromethane in poly(aryl-ether-ether-ketone). *J. Polym. Sci., Part B: Polym. Phys.* **1988**, *26*, 2145–2167.
13 Wolf, C. J.; Fu, H. Transport behavior of carbon disulfide into poly aryl ether ether ketone. *J. Polym. Sci., Part B: Polym. Phys.* **1996**, *34*, 717–724.
14 Mensitieri, G.; Delnobile, M. A.; Apicella, A.; Nicolais, L.; Garbassi, F. Solvent induced crystallization in poly(aryl-ether-ether-ketone). *J. Mater. Sci.* **1990**, *25*, 2963–2970.
15 Del Nobile, M. A.; Mensitieri, G.; Netti, P. A.; Nicolais, L. Anomalous diffusion in poly-ether-ether-ketone. *Chem. Eng. Sci.* **1994**, *49*, 633–644.
16 Arzak, A.; Eguiazábal, J. I.; Nazábal, J. Effects of methylene chloride sorption on the properties of poly(ether ether ketone). *J. Polym. Sci., Part B: Polym. Phys.* **1994**, *32*, 325–331.
17 Stober, E. J.; Seferis, J. C.; Keenan, J. D. Characterization and exposure of polyetheretherketone (PEEK) to fluid environments. *Polymer* **1984**, *25*, 1845–1852.
18 Seferis, J. C. Polyetheretherketone (PEEK): Processing-structure and properties studies for a matrix in high performance composites. *Polym. Compos.* **1986**, *7*, 158–169.
19 Hay, J. N.; Kemmish, D. J. Environmental-stress crack resistance of and absorption of low-molecular-weight penetrants by poly(aryl ether ether ketone). *Polymer* **1988**, *29*, 613–618.
20 Pérez-Martín, H.; Mackenzie, P.; Baidak, A.; Ó Brádaigh, C. M.; Ray, D. Crystallisation behaviour and morphological studies of PEKK and carbon fibre/PEKK composites. *Compos. Part A Appl. Sci. Manuf.* **2022,** *159*, 106992.
21 Zhang, J.; Liu, G.; An, P.; Yu, K.; Huang, J.; Gu, Y.; Yao, J.; Cao, R.; Liu, H.; Chen, C.; Zhang, C.; Wang, M. The effect of cooling rates on crystallization and low-velocity impact behaviour of carbon fibre reinforced poly(aryl ether ketone) composites. *Compos. B Eng*. **2023,** 254.
22 Gao, D.; Yang, H.; Liu, G.; Chen, C.; Yao, J.; Li, C. Effect of electrochemical oxidation degree of carbon fiber on the interfacial properties of carbon fiber-reinforced polyaryletherketone composites. *J. Reinf. Plast. Compos*. **2022**, DOI: 10.1177/07316844221145763.
23 Amedewovo, L.; Levy, A.; De Parscau du Plessix, B.; Orgéas, L.; Le Corre, S. Online characterization of moisture transport in a high-performance carbon fiber-reinforced thermoplastic composite at high temperatures: identification of diffusion kinetics. *Compos. B Eng.* **2023**, *256*, 110629.
24 Fieldson, G. T.; Barbari, T. A. The use of FTIR-ATR spectroscopy to characterize penetrant diffusion in polymers. *Polymer* **1993**, *34*, 1146–1153.
25 Yan, L. N.; Hou, L.; Sun, S. T.; Wu, P. Y. Dynamic diffusion of disperse dye in a polyethylene terephthalate film from an infrared spectroscopic perspective. *Ind. Eng. Chem. Res.* **2020**, *59*, 7398–7404.
26 Feng, K.; Hou, L.; Schoener, C. A.; Wu, P.; Gao, H. Exploring the drug migration process through ethyl cellulose-based films from infrared-spectral insights. *Eur. J. Pharm. Biopharm.* **2015**, *93*, 46–51.
27 Mensitieri, G.; Lavorgna, M.; Musto, P.; Ragosta, G. Water transport in densely crosslinked networks: a comparison between epoxy systems having different interactive characters. *Polymer* **2006**, *47*, 8326–8336.
28 Hong, S. U.; Barbari, T. A.; Sloan, J. M. Diffusion of methyl ethyl ketone in polysiobutylene: comparison of spectroscopic and gravimetric techniques. *J. Polym. Sci., Part B: Polym. Phys.* **1997**, *35*, 1261–1267.
29 Hou, L.; Feng, K.; Wu, P. Y.; Gao, H. Investigation of water diffusion process in ethyl cellulose-based films by attenuated total reflectance Fourier transform infrared spectroscopy and two-dimensional correlation analysis. *Cellulose* **2014**, *21*, 4009–4017.
30 Sammon, C.; Yarwood, J.; Everall, N. A FTIR-ATR study of liquid diffusion processes in PET films: comparison of water with simple alcohols. *Polymer* **2000**, *41*, 2521–2534.
31 Dong, Y.; Hou, L.; Wu, P. Exploring the diffusion behavior of urea aqueous solution in the viscose film by ATR-FTIR spectroscopy. *Cellulose* **2020**, *27*, 2403–2415.
32 International, A. ASTM D882: Standard test method for tensile properties of thin plastic sheeting. *Astm Standards* **2012,** 12.
33 Yang, X.; Wu, Y.; Wei, K.; Fang, W.; Sun, H. Non-isothermal crystallization kinetics of short glass fiber reinforced poly(ether ether ketone) composites. *Materials* **2018,** *11*, 2094.
34 Blundell, D. J.; Osborn, B. N. The morphology of poly(aryl-ether-ether-ketone). *Polymer* **1983**, *24*, 953–958.
35 Cebe, P.; Hong, S. D. Crystallization behaviour of poly(ether-ether-ketone). *Polymer* **1986**, *27*, 1183–1192.
36 Zhang, X. H.; Jiao, M. X.; Wang, X.; Li, B. L.; Zhang, F.; Li, Y. B.; Zhao, J. N.; Jin, H. H.; Yang, Y. Preheat compression molding for polyetherketoneketone: effect of molecular mobility. *Chinese J. Polym. Sci.* **2022**, *40*, 175–184.
37 Al Lafi, A. G.; Alzier, A.; Allaf, A. W. Wide angle X-ray diffraction patterns and 2D-correlation spectroscopy of crystallization in proton irradiated poly(ether ether ketone). *Heliyon* **2021**, *7*, e07306.

https://doi.org/10.1007/s10118-023-3046-8